PHASE I FINAL REPORT

DEVELOPMENT OF A WOVEN-GRID QUASI-BIPOLAR BATTERY

submitted to

Ballistic Missile Defense Organizational
Science and Technology
and
managed by

NASA Lewis Research Center
Procurement / MS 500-306
Cleveland, Ohio 44135-3191

by

AeroVironment Inc.
222 E. Huntington Drive, Ste. 200
Monrovia, CA 91016

January 1998

Abstract

Table of Contents

Section 1

INTRODUCTION

This report describes an analytical and experimental investigation of AeroVironment's Quasi-Bipolar battery concept. The analytical part of the investigation developed models for computing the current and voltage distributions, heat generation and transfer, cooling power requirements, etc. for the quasi-bipolar battery geometry.

A spreadsheet was written using the analytical results and empirical data to optimize the battery for thermal uniformity, given performance specifications, packaging, and other constraints. Quasi-bipolar battery packs were then designed for comparison with a state-of-the-art design hybrid electric vehicle battery pack.

The present modelling/battery design study demonstrates that there is a trade-off between thermal and specified electrical performance. Even with these tradeoffs, quasi-bipolar batteries can be designed that meet or exceed current state-of-the-art hybrid-electric vehicle battery pack electrical performance. At the same time, the battery configuration exhibits greater than ten times better thermal uniformity than state-of-the-art hybrid-electric battery packs. Thermal uniformity, power, and energy for these quasi-bipolar battery packs is projected to be very good. As shown below,

	Spiral Wound	*Max Energy Density*	*Min Thermal Variation*	*Optimistic Balanced*
Assumed Utilization of Active Materials (%)	33	33	33	50
Specific Power (W/kg)	500	500	1400	700
Power Density (W/L)	1600	1600	2500	1800
Specific Energy (Wh/kg)	29	39	33	47
Energy Density (Wh/L)	90	122	57	121
W-h battery/W-h AM (%)	54	72	60	68
Thermal dT (°C)	1.8	1.8	0.08	0.6

The batteries made from the 33% utilization active materials are representative of what can be achieved today. The optimistic balanced battery assumes a 50% utilization of the active materials. Values for the cell geometry were chosen to provide a balance between power, energy, and thermal uniformity.

The experimental part of the investigation demonstrated the concept of the quasi-bipolar plate applied to a lead foil current collector "grid" material wrapping around two sides of an inexpensive plastic film core. Approximately 50 quasi-biplate samples were fabricated using a hot laminating press. Fabrication of these plates was found to be relatively straightforward. Five of these plates were assembled into two cells plus one

two-cell battery. Data from these test cells were compared with existing data for similar true bipolar batteries. Formation and cycling of the battery caused the positive side of the plate to have a stress-corrosion problem where it was not protected by seal or active material. This problem was worst on the two cell battery where the biplate was not supported and allowed to droop around the edges. Adhesion with plastic is difficult, but hot lamination with "texture" between the plastic and lead shows some promise as a low cost method for fabricating the plates.

Section 2

BACKGROUND

A new high-power, high-voltage sealed, quasi-bipolar lead acid battery design is proposed for development. AeroVironment, Inc. is in the business of developing hybrid electric power and propulsion systems so the present investigation is geared toward that application. The quasi-bipolar battery concept, however, has a broad range of application.

The design provides a bipolar battery that uses fewer parts and is more easily assembled, thus providing a potentially less expensive battery. It also facilitates lateral heat transfer, permitting all battery cells to be laterally and uniformly cooled, and thereby operates at more uniform same temperatures. Thus, this battery can have great utility in high-voltage applications, such as in the propulsion of electric buses, cars, and forklifts.

The scope of this Phase I investigation was to address the feasibility of the method for making this electric battery.

The battery is composed of a plurality of cells which directly contribute to structural support. Each of these cells has elements which provide for gas and active material containment such that, following stacking of the plurality of cells along a battery axis, the stack is self-contained, and no casing external to the individual cells is necessary to prevent the leaking of gas, active material or electrolyte to the outside of the battery structure. According to this method, cells are produced by layering the biplate with a compliant sealing material on both sides to frame middle portions of each side which receive the active materials. Separator sheets lie between the layers of the stacks as assembled. During assembly, a gas-tight seal is created between each of the plates by the compliant sealing material. Thus, a self-contained battery stack is created which does not require an external casing, thereby providing for a lighter and less expensive battery.

This Phase I program also considered a quasi-bipolar battery for which each bipolar plate is constructed using a conductive material that is wrapped around a substrate utilized as the biplate. Use of this structure provides for easier battery construction, and allows for lateral heat transfer across each cell to the compliant sealing material, which acts in the stead of a casing. The compliant sealing material can transmit heat through the lateral sides of the battery, thereby allowing cooling of each cell by the battery exterior. In addition, the proposed battery also includes thermal insulators at both ends, and on the top and bottom ends, which block axial and vertical heat transfer through the end cells of the battery stack, thereby preventing the bipolar cells from operating at different temperatures.

Using this construction, all cells operate as close to the same temperature as possible and are cooled through the lateral sides of the battery, as facilitated by the thermally conductive current collector.

In full production, the anticipated advantages of this design, in comparison with other bipolar and quasi-bipolar designs include:

1. Low parts count. Only one bipolar plate per cell is used. The entire battery is a single integrated structure.
2. Seal periphery is minimized.
3. The quasi-bipolar biplate structure offers high conductivity/weight and low cost.
4. Plates can be horizontal thus minimizing acid stratification.
5. Mechanical compression enhances seal reliability and maintains active material to current collector "grid" contact.
6. Transverse heat flow ensures thermal uniformity
7. The structure is mechanically rugged
8. Final assembly is low-cost stacking operation amenable to automation.

2.1 Battery Structures

As used herein, the term "battery" refers to an electrochemical storage device that may consist of one or more chemical "cells" that each store electrical energy in the form of chemicals contained within the device. Typically, each cell includes three principal parts, including a positive electrode, a negative electrode and an electrolyte. The electrolyte is normally a liquid material, usually a relatively large molecule, that tends to dissociate or break-up into both positive and negative ions. The positive electrode is composed of a material that naturally reacts with the positive ions of the electrolyte, and requires free electrons for the reaction to proceed. On the other hand, the negative electrode is a material that naturally reacts with the negative ions, and so, must rid itself of extra electrons as the chemical reaction proceeds. In this manner, each of the positive and negative electrodes have an electron surplus or deficiency which gives rise to a voltage, or difference in charge, between the two electrodes.

Batteries are typically defined as using one of several conventional battery structures, which are generally either "monopolar" or "bipolar." The most common batteries are monopolar batteries, for example, a conventional, 12-volt lead-acid car battery. These batteries have six 2-volt cells that each use lead (Pb) as the negative active and lead-dioxide (PbO_2) as the positive active material, and sulfuric acid (H_2SO_4) as the electrolyte. Typically, monopolar configurations are useful for low-voltage applications, or where other factors, such as high-longevity, are paramount, but they are generally not well suited for high-voltage applications. For these applications, other conventional battery structures such as bipolar configurations are generally better suited.

The chemistry for charge and discharge is,

Negative (discharge)	$Pb+SO_4^{--}-2e^- \rightarrow PbSO_4$, and
Positive (charge)	$PbO_2+SO_4^{--}+4H^+ +2e^- \rightarrow PbSO_4+2H_2O$.

Distinguishing features of these various conventional battery structures will be discussed below.

- **Monopolar Batteries**

Monopolar Prismatic Structure

The monopolar prismatic structure is the conventional structure which is generally used for most commercial battery applications. This structure consists of a multiplicity of cells packaged in a single case structure and electrically connected in series with one another. In turn, each cell is composed of a stack consisting of a repeating sequence of a negative plate, a separator, a positive plate and another separator (the stack usually ends with a negative plate, such that the number of negative plates exceeds the number of positive plates by one). Tabs extending from each of negative plates are interconnected by a conductive bus which forms a negative terminus for each of the cells. Likewise, tabs extending from the positive plates are interconnected by a conductive bus which forms a positive terminus for each of the cells.

Each negative plate can consist of a conductive grid onto which negative active material is applied. The grid serves both as a current collector and as a mechanical support for the active material. Positive plates are similarly structured, except that positive active material is applied to the conductive grid. Both the negative and positive sides of the grid include integral projecting tabs, as discussed above. Conventional methods of grid fabrication include casting and expansion of thin sheet stock (*e.g.*, Optima punches rectangular holes into lead sheet). The expanded metal approach is generally used for high-volume, thin-plate applications, such as conventional car batteries.

The monopolar prismatic structure is suitable for a wide variety of applications. Its advantages include ease and low cost of manufacture. Its weaknesses include moderate Ohmic resistance associated with the grid and bus elements, and inability to accommodate extremely thin plate designs. It also suffers limitations in heat transfer, which become problematic for high-power applications. Each of these factors serve to limit the specific power capability of this structure. Another limitation of the structure is that active material is not as well "contained" as in other structures. This leads to reduced cycle life, especially in thin-plate, high-power applications.

The Monopolar Spiral-Wound Structure

The monopolar spiral-wound structure is similar to the prismatic version, except that only a single negative plate and a single positive plate (each having a punched, or an expanded metal grid) are wound over a central core. A pair of conventional separators is used to separate the plates. Termination is typically achieved via grid tabs, which extend axially outward and are welded to respective current collectors.

Advantages of this structure include reduced parts count (only two plates and two separators are used per cell), amenability to extremely thin (0.003") plates, good heat transfer, and improved active material containment. Possible disadvantages of the structure include reduced packaging efficiency due to the circular geometry, and the requirement that the battery cell be formed in-situ. With the requirement for cooling/heating of the battery, the packaging inefficiency becomes a virtue since this structure naturally provides flow paths and a large surface area for cooling.

The Tubular Structure

The tubular structure features positive (and occasionally negative) plates, where active materials are contained within a multiplicity of woven tubes. Each of these tubes has a central conductive "spine" which electrically and mechanically connects with a common metallic current collector.

The chief advantage of this battery structure is long cycle life which is due to relatively effective containment of the active materials. Disadvantages include high manufacturing cost, low specific power and low specific energy. The low energy and low power performance is due to the large plate thickness, which is inherent in the design of tubular structures.

The spiral-wrap structure, with its excellent containment, high-performance, and low-cost, appears to be displacing the tubular design in many applications.

Limitation of Monopolar Batteries

Monopolar cells are generally not suited for high-voltage, high-power applications. The numerous series and parallel connections that are required between monopolar cells are usually achieved by tapping connections at an end of each electrode; this increases the Ohmic resistance. The weight of separate enclosures for each cell of the monopolar battery, the liquid electrolyte and the inter-and intra-cell connections, all significantly increase the weight, complexity, and material cost of the battery. In addition, some designs also suffer from poor heat transfer.

To address many of these difficulties, bipolar battery configurations have been developed. With this configuration, electrodes of adjoining cells are on either side of a "biplate." The cells of the bipolar battery are thus simply layered in direct contact with one another, thereby providing large areas of interface and increasing charge mobility between cells.

The key point here is that the bipolar plate provides a very short current electronic path. This virtue is closely matched to the main problem – holes in the biplate also allow for a short ionic short circuit path. Since the bipolar cells contact each other directly, the required parts and the weight of the battery are both decreased. This tends to eliminate the need for current collectors corresponding to each electrode, and thereby tends to decrease battery weight, heat transfer problems and Ohmic resistance. Thus, conventional wisdom has it that bipolar configurations are better suited to high-voltage battery applications. Two different general types of bipolar structures are discussed below, namely, a "true bipolar" structure and our "quasi-bipolar" structure.

- **Bipolar Batteries**

The True Bipolar Structure

The true bipolar structure has a "stack" that employs a sequence of elements, including a monopolar negative plate, a separator, a repeating sequence of bipolar plates and separators, and a monopolar positive plate. Electrical termination is achieved via the monopolar end plates. Each of the bipolar plates consists of a thin, electronically conducting sheet (called a biplate) having negative active material applied to one side of its flat surface and positive material applied to the other side.

Since the electronic path is extremely short between the positive and negative active materials of adjacent cells (i.e., due the small thickness dimension of the biplate), the electronic component of resistance is typically very small. In contrast, the ionic component of resistance is often higher than with monopolar designs, since ionic currents typically flow only toward one face of the biplate, *i.e.,* toward a particular one of the active materials.

The advantages of a bipolar design is that low-resistance and high-power can be achieved for designs having plates of large lateral dimensions. Other advantages include inherently uniform current density over the surface of the plate, high-voltage production, good active material containment, the potential for eliminating grid materials, and potential ease of assembly.

The chief problems associate with the design of the true bipolar structure include corrosion stability of the biplate and difficulties in achieving a peripheral seal of the biplate. To date, these two problems have inhibited production of bipolar versions of the

lead-acid system, despite moderate development efforts which have extended over the entire century.

The Quasi-Bipolar Structure

"Quasi"-bipolar battery structures have been developed in an attempt to eliminate the corrosion problems which are present in the true bipolar design, and several quasi-bipolar battery designs currently exist. The common element for each is that a partitioned single biplate grid or conductor structure has negative active material applied over one region and positive active material applied over a separate region. Designs for these batteries have addressed both high- and low- power applications. Newer designs for these batteries have also utilized a particular woven grid structure (described below) which has a glass core, which is reported to make them highly resistant to corrosion.

In a high-voltage version of the quasi-bipolar battery, the "true bipolar" structure is simulated by the quasi-bipolar structure, in that a conductive material is wrapped around a non-conductive sheet. Individual bipolar plates formed by this process may thereafter be stacked to form a multi-cell structure. This approach side-steps some of the problems (i.e., high corrosion to the conductive biplate structure) associated with the biplate used in a true bipolar design, while it maintains most of the features of a true bipolar battery which are especially useful to high-power applications (e.g., high-voltage, low-electronic resistance, and use of stack assembly).

"Low-voltage" versions of the quasi-bipolar structure have also been under development. In one example, a grid element is divided into a left half and a right half. Negative material is applied to the left region, while positive material is applied to the right half region. Individual quasi-bipolar plates can then be stacked to achieve a multi-cell structure.

2.2 Conductor "Grid" Structures

- **Conventional**

Conventional battery grids are either cast, punched, or rolled yielding a lattice of lead upon and between which active material is applied. These designs can suffer positive plate corrosion problems for lead acid applications. In the case of cast grids, corrosion is enhanced by a combination of large crystal dimensions and surface imperfections. With expanded metal grids, corrosion problems are enhanced by stress concentrations due to the grid formation process itself. In both cases, there exists a mechanism called "stress corrosion" wherein corrosion is enhanced by concentrations of mechanical stress and vice versa (i.e., mechanical stress and corrosion couple in a negatively synergistic manner).

- **Woven Grid Structures**

A process has been recently developed and used in quasi-bipolar batteries, as indicated above, wherein lead (or an alloy of lead) is extruded over a fiberglass core to form a reinforced lead strand or yarn. Corrosion of this material is greatly reduced compared with both cast and expanded materials, for three primary reasons. First, the extrusion process itself establishes very small lead crystal domains, which inherently are corrosion resistant. Second, the surface of the extruded material is relatively smooth and without significant imperfections. Third, the fiberglass core is strong and provides good mechanical strength, and thereby de-couples the otherwise cooperating mechanisms of stress and corrosion.

Because of the high corrosion resistance of this coaxial, conductive material, thin, light-weight grid structures may be fabricated which simultaneously achieve long life, high specific energy and high specific power. This is achieved by weaving the lead yarn material to form a "scrim" type of material which can then be pasted with active materials. However, because of the difficulty of electrically terminating such scrims, conventional monopolar designs using woven grids are generally not practical. On the other hand, plates based on woven grids may be applied with moderate ease to quasi-bipolar design, since there is no requirement for current collection at a single point, except at the end monopolar plates.

While substantially reducing corrosion, quasi-bipolar designs which make use of this type of woven grid structure still are generally susceptible to leakage and corrosion at the edges of the individual battery cells. Further, as with the true bipolar and other batteries, these woven grid batteries still suffer heat transfer and cooling problems, as well as fabrication difficulties.

- **Lead Foil**

A lead foil current collector "grid" is simply a thin sheet of lead upon which the active materials are deposited. Conventional wisdom has it that this type of current collector structure should be plagued by corrosion problems. Recently however, lead-acid battery manufacturers have demonstrated long life and excellent good performance using such current collectors in both a spiral wound, and prismatic structure. Corrosion of the current collector material turns out not to be the primary cause of loss of battery life.

- **Quasi-bipolar Grid/Current Collector**

Any of the above grids can be employed in a quasi-bipolar structure. The original intent of this investigation (and hence the title) was to use, because of its superior corrosion resistance, the woven grid material discussed above. The present concept employs a lead foil conductor, wrapped around two sides of a plastic film, instead. This shift in position was encouraged by the realizations that the woven grid introduces significant challenges

costs to the manufacture process, and it appears that corrosion of lead foil grids is not a problem, as previously thought.

2.3 Battery Environment

For typical large scale applications, cells are packaged into modular housings, which in turn, are packaged into a "pack structure." Both the cost and mass for the sum of these packaging elements represents a significant fraction of the total.

Further added to this problem is the fact that battery cell performance is dependent upon temperature, which can differ between the individual cells within the battery stack. With a casing external to the battery cells, it becomes very difficult either to cool the battery to keep it at a preferred operating temperature, where it exhibits maximum efficiency, or to maintain a uniform operating temperature amongst the various individual cells of the battery. As with many chemical reactions, the battery cells operate most efficiently at a particular temperature, and deviation from this temperature by any of the cells results in reduced performance and/or reduced life. Battery cells are heated and cooled as they are charged and discharged and, consequently, cells at the middle of the stack may be experience a different temperature than cells at the ends. Further, improper temperature, or improper charging, can also cause the electrolyte and active materials to form gasses, which detracts from battery operation by removing needed materials from the chemical process, interfering with charge carrier migration, and by generating excess pressure. This problem may also require venting of the gasses from the cells.

To address this venting problem, individual cells are sometimes designed to have a pressure relief valve, which discharges gas pressure exceeding a predetermined amount. However, this adds components to each individual cell and significantly increases parts cost and assembly cost.

2.4 Manufacturing Considerations

Construction of batteries can be fairly intricate, and expense is directly related to the number of parts involved and the time required to assembly them. For example, where a casing is used external to the battery stack, to provide for containment of the electrolyte and active materials, the leak-proof status of the casing must be independently tested and assured. In addition, electrical connections are required to the end plates of the stacks so that current may be collected and supplied to the battery terminals. Typically, these connections require the manufacture of an appropriate current collector, which lies at either end of the battery stack and electrically couples output terminals of the battery to the finished stack. In the case of quasi-bipolar batteries, it is also typically necessary to independently place folded conductive material about opposite sides of the substrate while layering them, and further, independently heat-seal each cell's biplate to adjacent

separator plates. These complicated operations all contribute to added expense, and do not completely solve the problem of permitting uniform heat transfer.

There exists a definite need for a battery configuration that uses a minimal number of parts, is preferably inexpensive, and that is relatively easy to manufacture and assemble. Such a battery would contribute beneficially to reducing the costs of battery manufacture, and further, would be a positive step to producing affordable high-power electric batteries, such as could be applied to highway-speed electric vehicles. In addition, there exists a need for a light-weight battery that is relatively small in size, provides for improved cooling, and thereby produces power with heightened efficiency. Our invention satisfies these needs.

Section 3

PHASE I TECHNICAL OBJECTIVES

AeroVironment's proposed battery is based on an integrated concept wherein a single sealed high voltage "bipolar stack" is integrated with a battery tray and clamping bulkhead. As such, a single structure provides the desired system voltage and capacity; module to module inter-connects are eliminated and hold-downs are inherent. The design reduces "parts count" to a minimum while minimizing seal periphery and seal mass. This, in turn allows "deeper" seals without incurring significant cost, mass and size penalties.

The key objective of the AeroVironment design is a quasi-bipolar plate which registers and seals with adjacent glass-mat separators. In turn, each quasi-bipolar plate consists of a polypropylene (or other material) substrate sheet which is wrapped side to side with a "woven-grid" to provide electronic conductivity between the top and bottom substrate surfaces. A peripheral sealing frame is molded to each wrapped substrate.

One side of the bipolar plate is pasted with negative active material and the other side is pasted with positive active material. Conventional deep cycle processing is presently considered optimal; pasted plates are cured under controlled temperature-pressure-humidity cycles and cured bipolar plates are then in-situ or externally. Monopolar end-plates are constructed as above, except only positive or negative material is applied to one surface. The opposing surface is left unpasted; these surfaces contact with current collector sheets.

Separator elements are constructed from glass-mat (AGM) sheets to which a peripheral sealing frame is molded.

The complete battery is composed of a stack which is held together under compression by action of tie-rods or elastic membranes. The mechanical compression, besides effecting mechanical rigidity also effects frame-to-frame sealing and active material containment. Thermal insulation sheets are added to the structure which limit heat flow to the lateral dimension. This in turn provides "thermal symmetry" and encourages uniform active material temperature throughout the entire stack. End-stack thermal insulation is also added to prevent heat flow in or out of the stack ends.

From bottom to top, the stack elements are (see Figure 3.1)

1. Battery tray (113)
2. Tray thermal insulating sheet (153)
3. Bottom current collecting sheet (125)
4. Bottom monopolar plate (129)
5. Repeating sequence of:
6. Separator (131)
7. Bipolar plate (133)
8. Separator (131)
9. Top monopolar plate (135)
10. Top current collecting sheet (123)
11. Bulkhead thermal insulation (155)
12. Bulkhead (115)

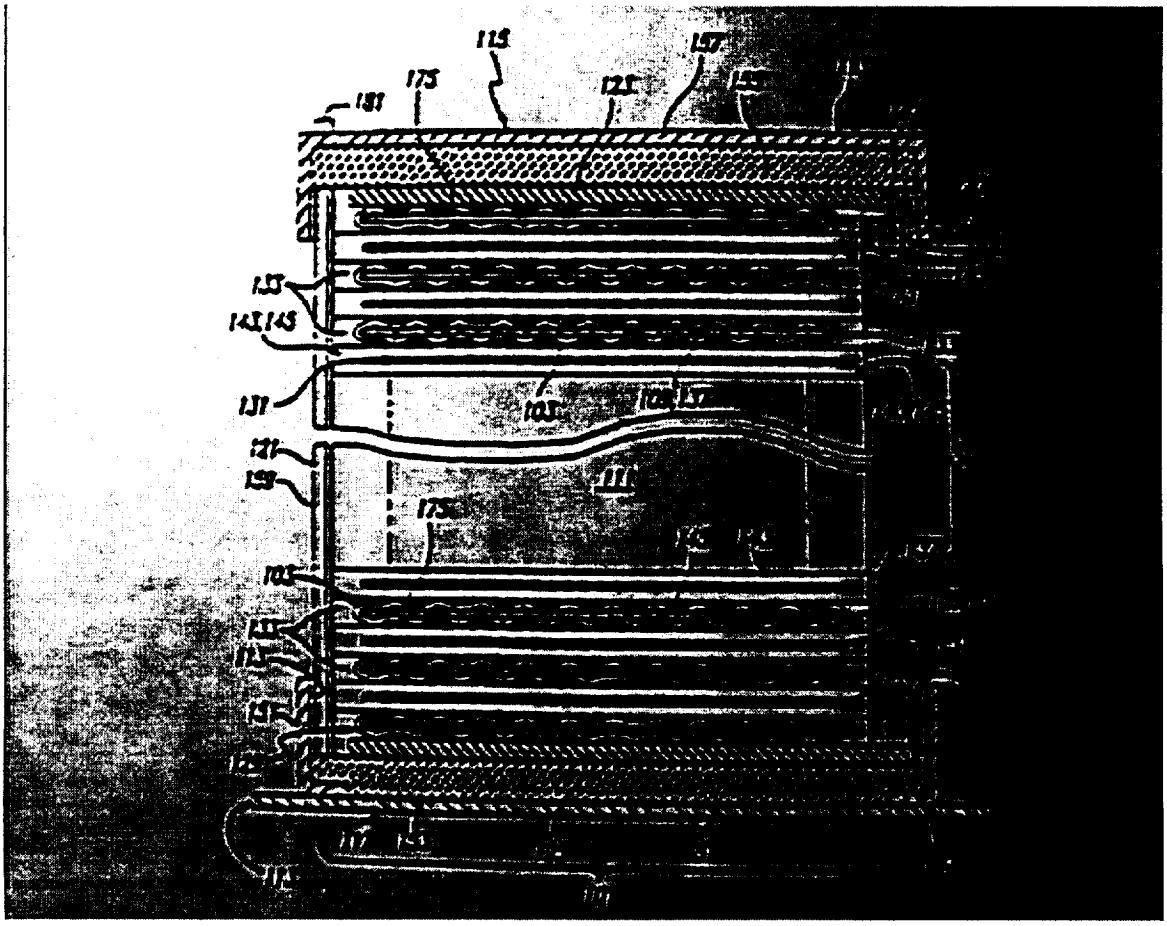

Figure 3.1 Figure of quasi-bipolar battery from AeroVironment Patent (5,441,824). Vertical tie rods are included which provide mechanical compression between the battery try and the bulkhead.

Gas management is achieved via channels and holes within the bipolar plate and separator frames. A single pressure relief valve is used for the entire stack. Miniature one-way flap valves may be integrated into the frame channels to prevent back-flow of water vapor and oxygen in the event that such is determined to be a problem. In either case, all cells will experience uniform venting pressure established by the single valve.

Current collecting sheets may be constructed from solder-coated aluminum. Electrical contact between the monopolar plates and the current collectors is maintained via mechanical pressure. Tabs which extend on the current collecting sheets are connected with female pin type connectors. By using multiple tables, stack current uniformity may be insured.

During stack assembly, electrolyte is added to positive plate surfaces and to separators in metered amounts; this approach is used to prevent negative plate oxidation.

The original Phase I objectives were to focus on high-risk sub-scale development of the lightweight energy storage system. Specific issues addressed by this Phase I research were:

- Analytical and numerical modeling of lead foil quasi-bipolar structure.
- Design of a battery appropriate for Hybrid Electric Vehicles, including modeling of heat generation and thermal management.
- Fabrication of lead foil biplates.
- Fabrication and preliminary testing of pasted biplates in single cells and 2 cell batteries.
- Visual inspection of quasi-biplate corrosion.

Section 4

ANALYTICAL RESULTS

An analytical evaluation of the quasi-bipolar battery geometry was performed. First, an analysis was performed of whether the quasi-bipolar stack makes sense, thermally, when compared with the spiral-wound geometry. A somewhat more involved description of the electrical and thermal properties of the battery were then developed for use in a design study.

Since the quasi-bipolar concept is, to some extent, a packaging concept that also solves the through-hole corrosion problem of true bipolar batteries, and not an innovation in the battery chemistry, an extrapolation, interpolation of the experimental data was employed in favor of sophisticated models for the active materials.

4.1 Thermal Uniformity for Stacked-Prismatic and Spiral-Wound Cells

The state-of-the-art in hybrid electric batteries is exemplified by a spiral wound battery structure, the product of Optima, Inc.. A figure of merit for the internal temperature uniformity within a single cell is the difference between the maximum and minimum temperatures. Thermal variations caused by the increase in coolant temperature along the cell are not considered here.

The temperature distribution with a quasi-bipolar stack and the spiral wound cell can both be approximated/idealized using a one-dimensional (rectangular and cylindrical respectively) approximation for the heat transfer equations, with uniform heat generation. A somewhat more realistic model for the quasi-bipolar battery as given later in this section.

We assume, in addition, that the heat flows along the lead foil direction in the prismatic geometry, and normal to it in the cylindrical geometry. The difference between the maximum and minimum temperatures for the cylindrical and prismatic geometries are then (Incropera and Dewitt 1981),

$$\Delta T_{\max,cyl} = \frac{\dot{q} R_{cyl}^{\,2}}{4\kappa_{\perp}}, \qquad \text{and} \qquad \Delta T_{\max,pris} = \frac{\dot{q} L_{pris}^{\,2}}{8\kappa_{\parallel}} \tag{4.1a,b}$$

where R_{cyl} is the cylinder radius, L_{pla} is the plate/conductor short dimension, $\dot{q}$ is the heating rate, $\kappa_{\perp}$ is the thermal conductivity in the normal direction (through the separator), and $\kappa_{\parallel}$ is the thermal conductivity in the parallel direction (along the plate).

If we roll-up a cell, then we can define an equivalence between the spiral-wound and prismatic cells, *i.e.*,

$$L_{cyl} = L_{pris}, \quad \text{and} \quad \tau_{pris} W_{pris} \sim \pi \; R_{cyl}^2, \tag{4.2a,b}$$

where W_{pris} is the plate long dimension, and τ_{pris} the cell thickness in the prismatic geometry.

The relative thermal uniformity of the cylindrical and prismatic geometries is given by,

$$\frac{\Delta T_{\max,cyl}}{\Delta T_{\max,pris}} = 2\left(\frac{R_{cyl}}{L_{pris}}\right)^2 \frac{\kappa_{\parallel}}{\kappa_{\perp}}. \tag{4.3}$$

For batteries with high active material to grid ratios, the thermal anisotropy is less dependent on the grid conductivity when compared with the thermal resistance of the electrolyte-filled separator and the positive (PbO_2) plate.

Presently, we use the thermal conductivity values for the fully charged battery. This is a reasonable approximation considering that batteries do not have a stellar utilization of the active materials. Using Russell's equation for porous media,

$$\frac{\kappa_{composite}}{k_{solid}} = \frac{\frac{\kappa_{liquid}}{k_{solid}} p^{2/3} + 1 - p^{2/3}}{\frac{\kappa_{liquid}}{k_{solid}}\left(p^{2/3} - p\right) + 1 - p^{2/3} + p}, \tag{4.4}$$

where p is the porosity, and computing the thermal conductivity of PbO_2 analytically (see Perry, 1973), using the equation for metal alloys,

$$k = \left(2.61 \times 10^{-8}\right)\frac{T}{r_{elect}} - \frac{\left(2 \times 10^{-17}\right)}{\rho \; c_p}\left(\frac{T}{r_{elect}}\right)^2 + \frac{97 c_p \rho^2}{MT}, \tag{4.5}$$

where T is in K, r_{elect} is the electrical resistivity in Ωcm, M is the molecular weight, c_p is in cal/gK, ρ is in g/cm^3, we approximate the following results (Table 4.1),

Separator+Acid	~ 1 W/mK	(95% porosity)
PbO2+Acid	~ 1 W/mK	(50% porosity)
Pb +Acid	~16 W/mK	(50% porosity)
Pb	~35 W/mK	(Grids)

Table 4.1 Thermal conductivities for various elements in a battery.

Using values representative of various battery geometries, the anisotropy of the thermal conductivities (including grid, active materials and separator) is roughly,

$$\frac{\kappa_{\parallel}}{\kappa_{\perp}} \sim 5 \text{ or } 6. \tag{4.6}$$

Plugging-in some round numbers, for the Optima Gen2 hybrid electric vehicle battery, we see that this plate size is better suited to being in the spiral wound than the quasi-bipolar structure, by a factor of two, *i.e.*,

$$\frac{\Delta T_{\max,cyl}}{\Delta T_{\max,pris}} = 2\left(\frac{R_{cyl}}{L_{cyl}}\right)^2 \frac{\kappa_{\parallel}}{\kappa_{\perp}} = 2\frac{\tau_{pris} W_{pris}}{\pi\ L_{pris}^2}\frac{\kappa_{\parallel}}{\kappa_{\perp}} \sim 2\left(\frac{2.5cm}{12cm}\right)^2 5.5 \sim 0.5 \tag{4.7}$$

Clearly, for a plate that is very narrow and long, *i.e.*, with L_{pris} short and W_{pris} long, the prismatic structure can have better thermal uniformity. This geometry has the additional benefit of having a shorter electrical path from cell to cell, and better current uniformity. In contrast, the taller cylindrical cell yields better (1D) thermal uniformity, but at the expense of having longer electrical paths from cell to cell, and worse current uniformity.

By way of example, The current design optimizations called for relatively longer plates which reverses the advantage, *i.e.*,

$$\frac{\Delta T_{\max,cyl}}{\Delta T_{\max,pris}} = 2\frac{\tau_{pris} W_{pris}}{\pi\ L_{pris}^2}\frac{\kappa_{\parallel}}{\kappa_{\perp}} \sim 2\frac{(0.25cm)(120cm)}{\pi\ (8.5cm)^2} 5.5 \sim 1.5, \tag{4.8}$$

The cylindrical cell can also often have an advantage over a prismatic stack (without cooling fins) when considering convection cooling of the surface. The ratio of the heat transfer area for the two geometries is,

$$\frac{A_{cyl}}{A_{pris}} = \frac{2\pi R_{cyl} L_{cyl}}{2\tau_{pris} W_{pris}}, \tag{4.9}$$

where $\tau_{prismatic}$ is the cell thickness in the prismatic geometry. Again, narrow, long plates are what's indicated for the prismatic cells.

4.2 Macroscopic Battery Description

Using the simple macroscopic battery model,

$$v_{cell} = V_0 - R_{cell} i_{cell} \tag{4.12}$$

$$i_{cell} = \frac{V_0}{2R_{cell}}\left(1 \pm \sqrt{1-\varepsilon}\right) \tag{4.13}$$

where,

$$\varepsilon = \frac{4R_{cell}P}{V_0^2} = \frac{P}{P_{\max}} \tag{4.14}$$

is the ratio of the cell power, P, at the current, i_{cell}, to the theoretical maximum ($V_0/2$) cell power output, $P_{\max}$, v_{cell} is the cell voltage, V_0 is the open circuit voltage, and R_{cell} is the cell's internal resistance. Note that on charge ($i_{cell} < 0$), V_0 is slightly larger, and R_{cell} roughly double, the values for discharge ($i_{cell} > 0$).

The corresponding Ohmic internal heat generation can be written as,

$$Q_{Ohmic} = i_{cell}^2 R_{cell} = \frac{V_0^2}{4R_{cell}}\left(1-\sqrt{1-\varepsilon}\right)^2 = V_0 i_{cell} - P = \frac{V_0^2}{2R_{cell}}\left(1-\sqrt{1-\varepsilon}\right) - P. \tag{4.15}$$

For small ε this becomes:

$$Q_{Ohmic} \approx \frac{\varepsilon}{4}P = \frac{R_{cell}}{V_0^2}P^2 . \tag{4.16}$$

The macroscopic heat absorbed owing to the chemical reaction is reversible, and given by,

$$Q_H = -i_{cell} T\left(\frac{dV_0}{dT}\right)_p , \tag{4.17}$$

where $T\left(\frac{dV_0}{dT}\right)_p$ varies from approximately 0.00 V at full charge to 0.03 V near the end of discharge and is around 0.02 V at 50% state of charge (at 313K). Since much of the

battery cycling is spent at around 50% state of charge, using a constant value of 0.02 V is not unreasonable.

4.3 Current Distribution and Potential in Quasi Bipolar (QB) Plates

In this analysis, which follows Rippel (1994), the battery is separated into two regions, the "effective" quasi-biplate in which the current is taken to flow along the lead foil direction, and the "effective" separator in which the current flows normal to the lead foil. Mostly, the effect of the active materials are grouped with the separator. The voltage gradient along the grid is,

$$\frac{dv}{dx} = \frac{-r_g}{\tau_g W} i, \tag{4.18}$$

where v is the local voltage, W is the grid dimension normal to the current flow, r_g is the effective grid resistivity, τ_g is the effective grid thickness, and i is the current along the grid.

$$\frac{di}{dx} = (V_0 - v)\frac{W}{\tau_s r_s}. \tag{4.19}$$

Solving the above system of equations yields a current distribution *along the grid.* For the dual wrap-around configuration this is (note: half the cell current flows around each side).

$$\frac{i(\xi)}{i_{cell}} = \frac{1}{2}\frac{\sinh(\lambda\xi)}{\sinh(\lambda)}, \tag{4.20}$$

where

$$\lambda^2 = \frac{r_g}{r_s}\frac{\ell^2}{\tau_g \tau_s} \tag{4.12}$$

is a quasi-bipolar cell geometry parameter, $\xi = \frac{x}{\ell}$ is the normalized distance from the center of the plate, $\ell = \frac{L}{2}$ is the plate half-width, r_s is the effective separator resistivity, and τ_s is the effective separator thickness. Large values of λ correspond to a cell where grid resistance dominates, and a small value corresponds to the case were separator resistance dominates.

The current density distribution in the normal direction through the separator is:

$$\frac{di}{dx} = \frac{i_{cell}}{L}\frac{\lambda}{\tanh\lambda}\frac{\cosh(\lambda\xi)}{\cosh\lambda}, \tag{4.13}$$

and the ratio of the minimum to maximum current density is then:

$$\frac{\left(di/dx\right)_{\min}}{\left(di/dx\right)_{\max}} = \frac{1}{\cosh\lambda}. \tag{4.14}$$

Noting that the macroscopic cell voltage (at the edges of the plate) is,

$$v_{cell} = V_0 - R_{cell} i_{cell}, \tag{4.15}$$

we can write for the potential distribution,

$$v(\xi) = V_0 - R_{cell} i_{cell}\frac{\cosh(\lambda\xi)}{\cosh\lambda}, \tag{4.16}$$

where

$$R_{cell} = R_s\frac{\lambda}{\tanh\lambda} \tag{4.17}$$

is the macroscopic cell resistance, and

$$R_s = \frac{\tau_s r_s}{WL} \tag{4.18}$$

is the "bulk" resistance of the cell's effective separator. The maximum potential difference on the separator is then,

$$\Delta V = R_{cell} i_{cell}\left(1 - \frac{1}{\cosh\lambda}\right). \tag{4.19}$$

For a representative spiral-wound battery, (ignoring the electrical conductivity of the active material along the grid), we have roughly,

$$\lambda^2 = \frac{r_g}{r_s}\frac{\ell^2}{\tau_g\tau_s} < \frac{10^{-5}\Omega cm}{2.8\Omega cm}\frac{(12cm)^2}{0.022cm\times 0.3cm} \sim 0.25^2. \tag{4.20}$$

From Equation 4.17 above we see that,

$$\frac{R_s}{R_{cell}} > 0.98, \tag{4.21}$$

which shows that only a fraction (not including the interconnects) of the cell resistance is in the grid, *i.e.*, 98% of the resistance is in the separator and active materials.

4.4 Differential Equations for Heat Transfer in 1-D Prismatic QB Stack

In this analysis, as with the electrical model above, the model considers the "effective" separator and grid, denoted by the subscript "*g*" for the effective grid and "*s*" for the effective separator. The active material values are lumped-in with the grid and separator parts of the battery. In addition, the heat capacity of the grid are lumped-in with the heat capacity of the effective separator, and the thermal conduction of the effective separator is lumped-in with the grid.

For a differential volume of the battery span, the local Ohmic heating is divided into two parts, the local Ohmic heating of grid,

$$dq_g = 2\frac{i^2 r_g}{W\tau_g}\ell\frac{dx}{\ell} = i_{cell}^2 R_{sep} 2\lambda^2 \frac{\sinh^2\lambda\xi}{\sinh^2\lambda}\frac{d\xi}{2}, \tag{4.21}$$

and the local Ohmic heating of separator,

$$dq_s = \left(\frac{di}{dx}\right)^2 \frac{r_s\tau_s}{W}\frac{1}{2}\ell\frac{dx}{\ell} = i_{cell}^2 R_{sep}\left(\frac{\lambda}{\tanh\lambda}\right)^2 \frac{\cosh^2\lambda\xi}{\cosh^2\lambda}\frac{d\xi}{2}. \tag{4.22}$$

Since most high performance batteries will have $\lambda < 0.5$, we can get a better feel for the heat generation by using a small λ approximation.

$$dq_g \sim i_{cell}^2 R_{sep} 2\sinh^2\lambda\xi\frac{d\xi}{2} \sim 0 \tag{4.23}$$

$$dq_s \sim i_{cell}^2 R_{sep}\frac{d\xi}{2} \tag{4.24}$$

The net local Ohmic heating is then,

$$dq_g + dq_s = i_{cell}^2 R_{cell}\frac{d\xi}{2}\frac{\tanh\lambda}{\lambda}\left(\frac{\lambda}{\sinh\lambda}\right)^2\left(1+3\sinh^2\lambda\xi\right) \sim i_{cell}^2 R_{cell}\frac{d\xi}{2}. \tag{4.25}$$

The remaining terms in the heat transfer equation involve the heat created/absorbed by chemical reaction,

$$dq_h = -\left(\frac{di}{dx}\right)T\left(\frac{dE}{dT}\right)_p \ell\frac{dx}{\ell} = -\frac{i_{cell}}{2}\frac{\lambda}{\tanh\lambda}\frac{\cosh\lambda\xi}{\cosh\lambda}T\left(\frac{dE}{dT}\right)_p d\xi \sim -\frac{i_{cell}}{2}T\left(\frac{dE}{dT}\right)_p d\xi \tag{4.26}$$

the heat storage,

$$dq_t = 2\rho_s c_{p,s}\tau_s W\frac{\partial T}{\partial t}\ell\ \frac{d\xi}{2}, \tag{4.27}$$

and the heat conduction,

$$dq_c = 4\kappa_g W\tau_g\frac{\partial^2 T}{\partial \xi^2}\frac{1}{\ell}\frac{d\xi}{2}. \tag{4.28}$$

The 1-D heat transfer equation is then:

$$dq_t = dq_c + dq_g + dq_s + dq_h \tag{4.29}$$

To indicate the relative importance of the Ohmic and chemical heating, the heat generation terms can be combined as,

$$dq = \frac{i_{cell}}{2}\frac{\lambda}{\sinh\lambda}\left\{i_{cell}R_{cell}\frac{1}{\cosh\lambda}\left[1+3\sinh^2\lambda\xi\right]-T\left(\frac{dE}{dT}\right)_p\cosh(\lambda\xi)\right\}d\xi$$
$$\sim\frac{i_{cell}}{2}\left\{i_{cell}R_{cell}-T\left(\frac{dE}{dT}\right)_p\right\}d\xi. \tag{4.30}$$

Since the thermal diffusion time scale of the system,

$$t_T = \frac{\ell^2}{2}\frac{\rho_s c_{p,s}\tau_s}{\kappa_g\tau_g} \sim \frac{(5cm)^2}{2}\frac{3\frac{J}{cm^3K}0.3cm}{0.35\frac{W}{cmK}0.015cm} \sim 35 \text{ minutes.} \tag{4.31}$$

is large, it is simpler to consider the storage and diffusion parts of the equation separately.

- **Steady State Heat Transfer**

The first order steady state heat transfer equation (omitting higher order terms) is,

$$\frac{d^2T}{d\xi^2} = Q_{cell}\frac{\ell}{4W\kappa_g\tau_g}, \tag{4.32}$$

where

$$Q_{cell} = i_{cell}\left\{i_{cell}R_{cell} - T\left(\frac{dE}{dT}\right)_p\right\} \tag{4.33}$$

The difference between the centerline and seal temperature is found by integrating this equation twice, *i.e.*,

$$\Delta T_{cell} = \frac{Q_{cell}}{2}\frac{1}{2\kappa_g}\frac{\ell}{W(2\tau_g)}. \tag{4.34}$$

This can also be written in terms of an effective mean conductivity, $\kappa_{\|,cell}$, and total cell thickness, τ_{cell}, as,

$$\Delta T_{cell} = \frac{Q_{cell}}{4}\frac{1}{\kappa_{\|,ce;;}}\frac{\ell}{W\tau_{cell}}. \tag{4.35}$$

- **Transient Response**

Higher order and spatial terms are omitted to yield the transient response, which can again also be written in terms of mean cell quantities,

$$\frac{dT}{dt} = \frac{Q_{cell}}{\rho_s c_{p,s}\tau_s WL} = \frac{Q_{cell}}{(\rho_s c_p)_{cell}\tau_{cell}WL} \tag{4.36}$$

4.5 External Cooling of Cell

The minimum volumetric flow rate of coolant, $\dot{V}_{cool}$, is given by,

$$\dot{V}_{cool} = \frac{Q_{cell}}{\rho_{cool}c_{p,cool}\Delta T_{cool}}, \tag{4.37}$$

where Q_{cell} is the average heat generated by the cell, ΔT_{cool} is the mean difference between the inlet and outlet temperatures of the coolant, ρ_{cool} is the coolant density, and $c_{p,cool}$ is the specific heat. A given temperature drop requirement dictates the minimum flow rate, independent of the particular battery geometry.

The particular geometry does, however, determine the power required to move the coolant past the batteries.

For roughly constant density flow, an approximation to Kayes and London (1964) for the pressure drop through a heat exchanger with inlet and exit contraction and expansion is,

$$\Delta P = \frac{G^2}{2\rho}\left[K + f\frac{A_s}{A_c}\right] \tag{4.38}$$

where K is a contraction/expansion pressure-loss coefficient that ranges from 2.2 for large contractions to zero for no contraction, and f is the friction factor,

$$f = \frac{\rho\tau_0}{G^2/2}, \tag{4.39}$$

which is correlated as a function of Reynolds number,

$$\mathrm{Re} = \frac{4r_h G}{\mu}. \tag{4.40}$$

The power required to pump the coolant through the heat exchanger is then (again for small variations in fluid density),

$$Pwr = \Delta P\ \dot{V}, \tag{4.41}$$

where $\dot{V}$ volumetric is the flow rate.

In the present investigations, the friction factor and heat transfer coefficients are interpolated from graphs for flow between parallel plates insulated on one side (Kayes and London, 1964).

Neglecting the heat absorbed in the chemical reaction, we approximate for the heat generation within the cell, (note that R is a function of the charge/discharge rate),

$$Q_{cell} \sim Q_{Ohmic} \sim \frac{R_{cell}}{V_0^2} P^2. \tag{4.42}$$

The end of the plate has a convection boundary condition (assuming $\dot{m}c_p$ is large enough), of

$$Q_{cool} \sim Q_{Ohmic} \sim \frac{R_{cell}}{V_0^{\,2}} P^2 \sim 2hA_s \Delta T_{cool} \tag{4.43}$$

where A_s is the heat transfer surface area per cell.

4.6 Cell Paste Parameters

The model requires empirical data for the cell resistivity, density, Amp-hour density, etc. The numbers in Table 4.2 below, which includes the separator volume and mass, lists the estimated data for the Optima Gen2 battery (used in the design of the QB battery stack in the present study), compared with the Arias Research Associates (ARA) pasted used in the present test batteries, and a hypothetical "higher utilization" paste.

	Optima ~Gen2	Arias Bipolar	High Utilization
Resistivity (Ω-cm)	2.7	2.6	2.7
Density (g/cm^3)	3.1	2.7	2.6
A-h density (A-h/kg)	26.5	22.8	34.0
Implied Utilization	33%	29%	50%

Table 4.2 Cell parameters for use in the battery design.

Section 5

EXPERIMENTAL RESULTS

The experimental portion of this investigation was primarily aimed at gaining experience in the construction of quasi-biplates of lead foil wrapped around lead film. Approximately 50 plates were produced using a hot laminating plate. Several of the "best" plates were assembled into test cells by Arias Research Associates. The cells were formed into working batteries and some testing was performed by ARA. The test cells were torn down for a visual inspection of the plates.

5.1 Hot Laminating of Plates

For the Phase I program, the grid material for the biplates was originally intended to be made from a woven lead/glass grid material. The reason for using this material was for its claimed superior resistance to corrosion. Recently, batteries employing thin foil grids, from Bolder Technologies Corporation and Portable Energy Products (PEP), have been reported to exhibit acceptable life and corrosion performance.

Construction of a quasi-bipolar plate using lead foil is anticipated to be far simpler and cheaper than using a woven grid. In view of the success of the above batteries, lead foil wrapped around plastic film cores was chosen for a quasi-bipolar plate. This type of biplate, when used with peripheral seals, also falls within the current AeroVironment patent.

Approximately 50 biplates were formed by wrapping (0.005" thick) lead foil sheets around various inexpensive types of plastic/composite (0.005" thick) film material. After hot laminating, the plate thicknesses ended up being in the range of 0.015"-0.017." This construction was then put into a hot laminating press subject to various temperatures (440-500°F), pressures (200-600psi), and times (0.5-30sec). In this range, temperature seemed to be the most important parameter.

Four types of low cost laminating plastics were used in the study: polypropylene (PP), polyethylene (HDPE), polyester (Mylar/PET), and polyvinyl chloride (PVC). For some of the plates, fiberglass of microporous pasting paper was also melted into the plastic film between within the lead foil. Of the plastics, the polyester film appeared to have the best adhesion. This adhesion was improved with the addition of microglass pasting paper.

The PP, HDPE, and polyester films were amenable to hot laminating, at the temperatures and pressures used in this study, the PVC, however, burnt with an unpleasant odor. Of the three other candidates, the polyester film exhibited surprisingly good adhesion to the lead. Polyester film was used in the test biplates, because it was felt that some adhesion would help to retard the wicking of the acid between the lead foil and the plastic film.

One problem that was observed when hot laminating the biplates was a "blowout" of the hot melted plastic through the fold in the lead sheet (see Figure 5.1). This blowout was later controlled, initially, by limiting the travel of the hot laminating press using ad-hoc shims or with fiberglass fabric between the lead foil sheets. Later, it was found that the blowout could be eliminated by limiting the temperature to just above the melting temperature of the plastic film. A better solution is to design a fixture dedicated to making these plates.

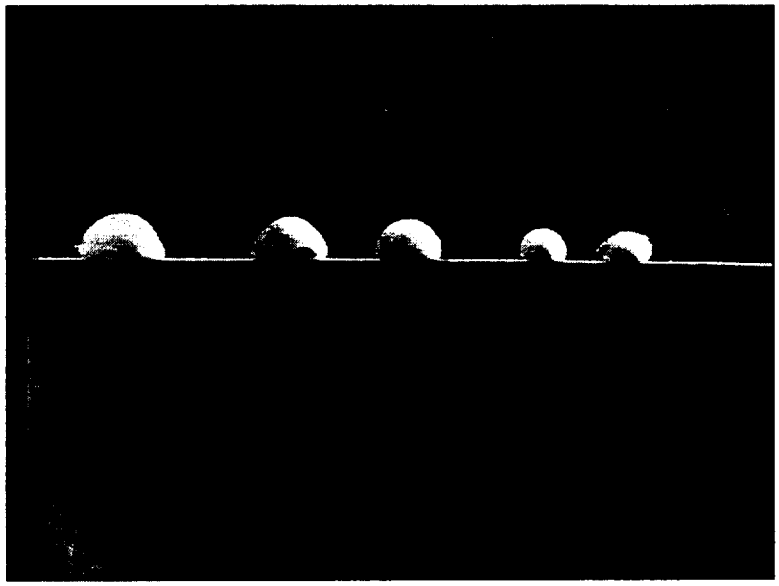

Figure 5.1 Blow-out of polypropylene plastic film through fold in lead foil.

Lowering the laminating temperature had the benefit of limiting bubble production in the plastic but at the expense of reducing the strength of the lead-plastic bond. Since the bubbles were "closed cell" we did not worry about them too much.

An unexpected plus of the hot laminating process was that the overlap/seam of the lead sheet on the one side of the biplate was fused by the heat and pressure (see Figure 5.2). Note that this seam did not pose a corrosion problem in the test cells, and in fact was hard to see.

Figure 5.3 illustrates bubble formation that occurred in all of the test plates. In this case, the lead foil was peeled back from a polyester film sample. Note also that there was sufficient adhesion with the polyester film to cause failure of the lead foil during the peel-back.

Figure 5.4 is a peel-back of lead foil from a polyester film/microglass pasting paper composite. This combination was produced by layering the polyester and pasting paper

inside the (wrapped-around) lead foil prior to applying heat and pressure. This combination offered the best adhesion.

Figure 5.5 illustrates an experiment where woven fiberglass fabric was added to polypropylene to limit the travel of the press to prevent blow-out, which it did, and to increase adhesion, which it did not.

A single test biplate was prepared with PVC for the core material. The temperature of the laminating press was 100°C too high for this plastic and it burned with an acrid odor.

A potential negative of the hot laminating process is that may introduce large stresses into the lead foil material. In the long run, this can cause stress-corrosion and a loss of battery life. For this reason, more thorough testing and an examination of other options will need to be performed before committing to this type of biplate.

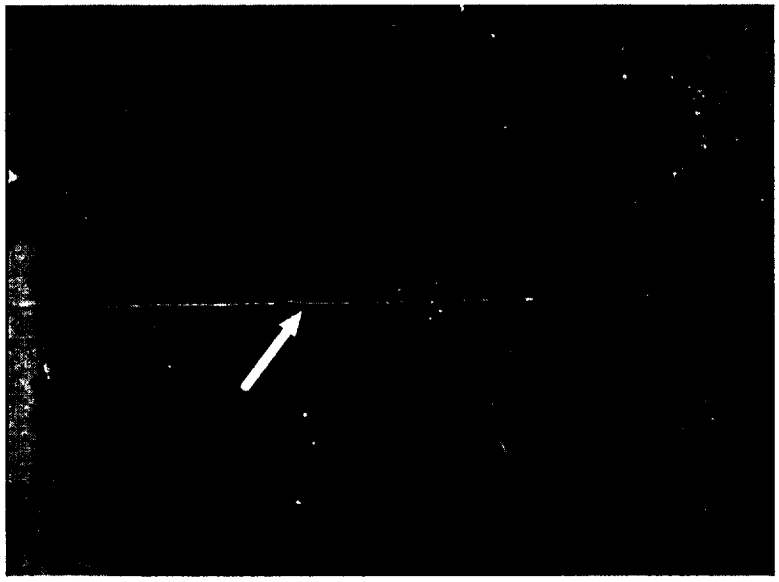

Figure 5.2 Overlap/seal in lead sheet performed during hot laminating process. The arrow points to the edge of the overlap/seal.

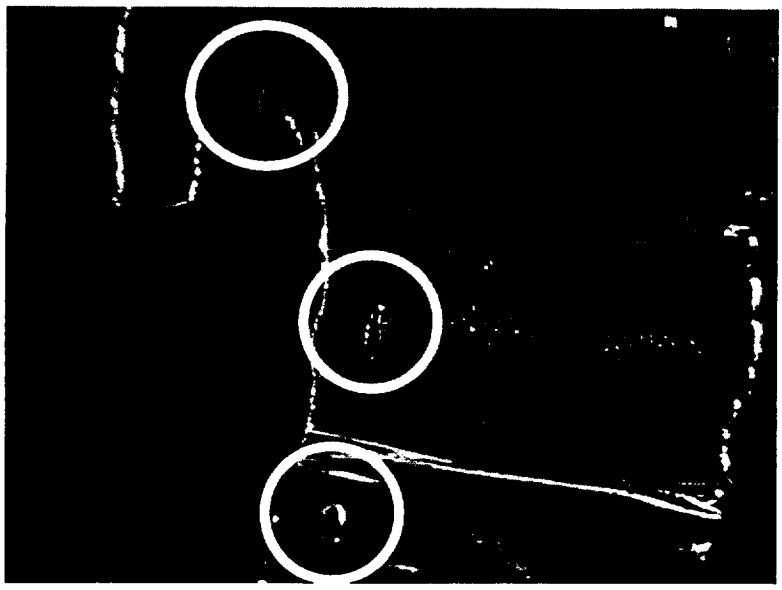

Figure 5.3 Peel-back of lead foil from polyester film demonstrating bubble formation and adhesion of lead foil to film. The circles mark a small piece of the lead foil that remained stuck to the polyester during peeling.

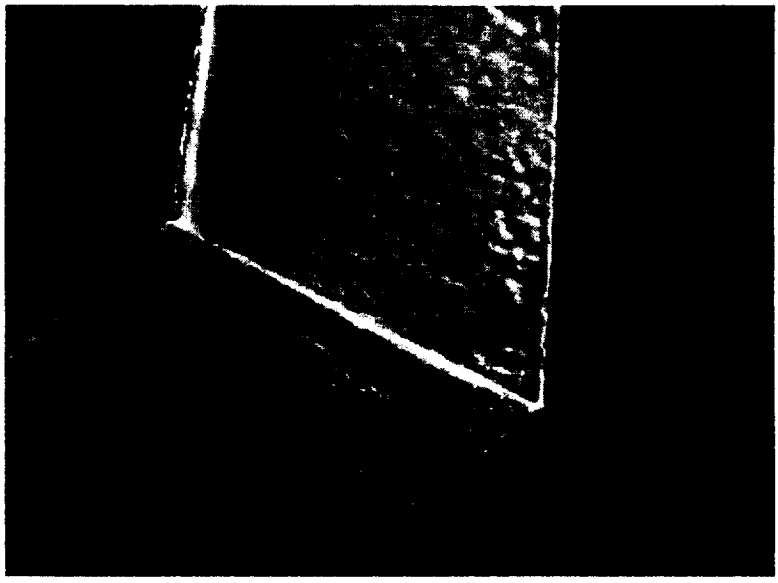

Figure 5.4 Polyester/microglass pasting paper composite. Adhesion (noticeable peel resistance) was observed. Failure of composite before bond was observed.

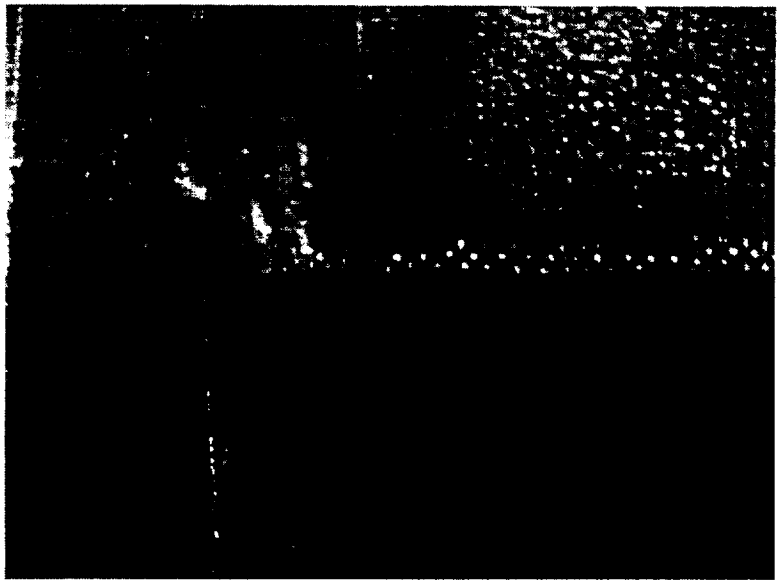

Figure 5.5 Polypropylene/fiberglass composite (top). No significant adhesion, but mechanical texturing of the lead foil (lower half) was observed.

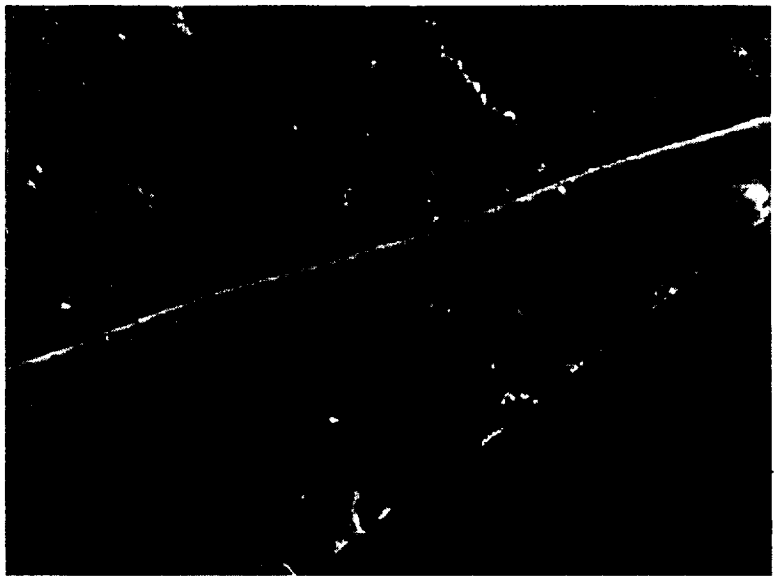

Figure 5.6 Peel-back of PVC test plate. This plate burned with an acrid odor in the in the laminating press.

5.2 Test Cells

Two single cell, and one 2 cell battery, using the above quasi-biplates, were assembled and tested at Arias Research Associates. The purpose was to have a first look at how the quasi-biplates faired in a real battery environment. A partially dissembled two cell test fixture is shown in Figure 5.7. The compression mechanism is shown in the foreground, and the outer casing is shown in the background. With the exception of the quasi-biplates, the construction of the cells were identical, including the lack of peripheral seals, to the true bipolar battery test cells produced by ARA.

Figure 5.7 Arias Research Associates standard test cell. Partially dissembled, outer case and lid is seen in the background.

Test results for the present batteries are summarized below. The test cells had similar capacity to ARA's own bipolar test cells (see Table 5.1). However, while the single cells were reported to have similar performance to their standard cell, the two cell battery had some difficulty on formation. The resistance and open circuit voltage shown in Table 5.1 show the problem. Visual inspection during tear-down revealed significant corrosion around the periphery of that positive active material of the biplate and this is a possible contributing factor.

Figure 5.8 is a plot of discharge time *vs.* current for the quasi-bipolar test cells. The exponent of a least-squares power law fit to the data for the single cells is approximately -0.88.

From this data the bulk cell (including the separator, but including the supporting lead conductor "grid") density is 2.6 g/cm^3 for the quasi-bipolar cells and 2.7 g/cm^3 for the ARA standard, and a specific Amp-hour capacity of 20 A-h/kg for test cells and the 22.8 A-h/kg for the standard. These numbers are not exceptional and represent a utilization of less than 30%.

The test cells did not appear to be holding-up too well under cycling, so further testing of the cells was not performed. During the tear-down inspection, inconsistent resistances (reported in Table 5.1) were measured across the test cells.

ARA's observations of the tear-down indicated that the active materials appeared to be properly formed, without sulfation. The active materials on one of the single test cells, however, appeared to have had some charge reversal indicated by some pinkness of the negative plate. This may point to a short somewhere in the cell.

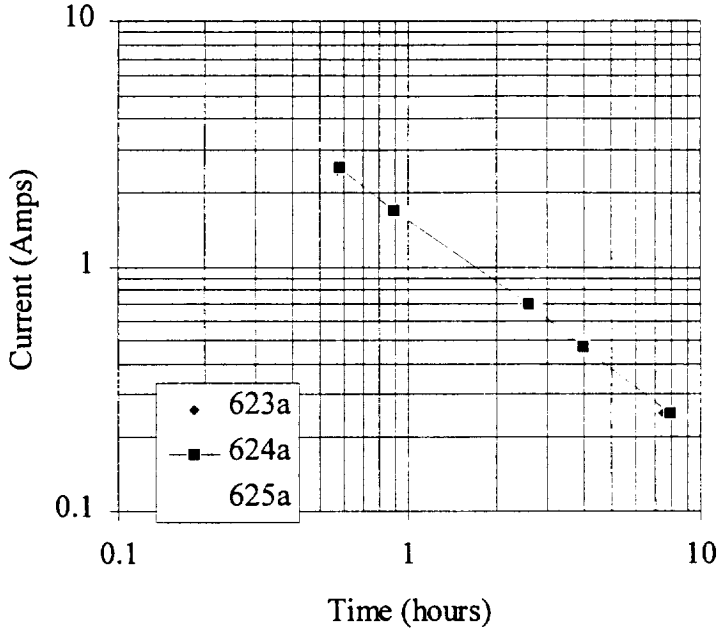

Figure 5.8 Discharge Time vs. Discharge Time for Quasi-bipolar test cells. The exponent of a least-squares power law fit to the data for the single cells is approximately -0.88.

Cell ID	623a	624a	625a	ARA Standard
Volts	2	2	4	2
Paste Area (cm^2)	48	48	48	48
PAM Thickness as pasted (1/1000")	85	91	87	86
NAM Thickness as pasted (1/1000")	79	74	80	72
Separator Thickness (1/1000")	72	72	72	72
Total Thickness (cm)	0.60	0.60	0.61	0.58
PAM + NAM Volume(cm^3)	28.8	28.8	29.3	27.8
PAM mass (g)	34.9	34.9	34.8	34.5
NAM mass (g)	26.6	26.6	26.6	26.5
Separator (g)	2.6	2.6	2.6	2.6
Electrolyte (g)	11.6	11.6	11.6	11.6
H_2O loss during formation (g)	0.8	0.8	0.8	0.8
Total Mass (g)	74.9	75.0	74.8	74.4
Average Density (g/cm^3)	2.6	2.6	2.6	2.7
Capacity @ C/1 (Ah)	1.43	1.43	1.64	1.70
Energy @ C/1 (Wh)	2.7	2.7	3.2	3.3
Specific Energy per cell @ C/1 (Wh/kg)	37	36	42	45
Resistance measured during autopsy (cell 1/2,cell 2/2)	64mΩ	18mΩ	1.1Ω, 19Ω	-
Open Circuit Voltage Volts (cell 1/2, cell 2/2)	1.919	2.031	1.246, 0.712	-

Table 5.1 Performance data on cells with quasi-bipolar plates compared with ARA's "standard" cell. Masses and specific energies do not include the battery case and "grid," but do include the separator.

5.3 Tear-Down Inspection of Quasi-bipolar Plates

Test cells were disassembled and a visual inspection of the cells was made. The results were promising. On the plus side some adhesion of the polyester + microglass pasting paper was observed (Figure 5.8). In addition, the expected corrosion of overlap seam/weld and of the fold in the biplate did not occur (see Figure 5.11). On the down side, the interaction of the lead foil, PbO_2, and sulfuric acid caused the lead foil to delaminate and bulge; this caused a stress-corrosion feedback mechanism and significant corrosion around the periphery of the positive active material. The worst case we saw was for the two cell battery, illustrated in Figures 5.9 and 5.10. No particular care was taken in the choice and conditioning of the lead foil, and the present quasi-bipolar design specifies seals over this region of the plate. Corrosion at this location should have been an issue in the Bolder and PEP batteries, so some collaboration with them may make sense if this concept is further developed.

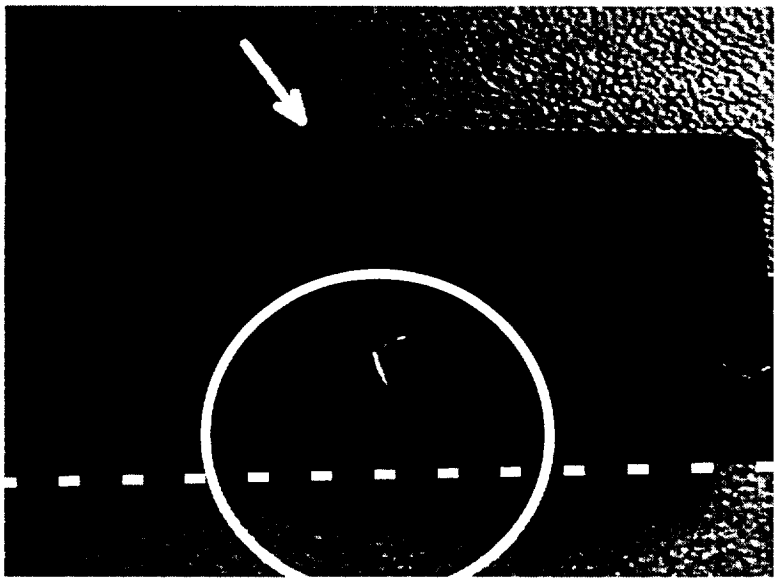

Figure 5.8 Inside view of lead foil sample from 2V test cell, peeled away from polyester/micro glass pasting paper core. The white circle marks a region where adhesion was maintained and the lead sheet was unaffected by the acid. It's not apparent from the photograph, but this region is shiny metallic. The arrow marks where the fold in the lead was. The plate was cut in half along the dashed line.

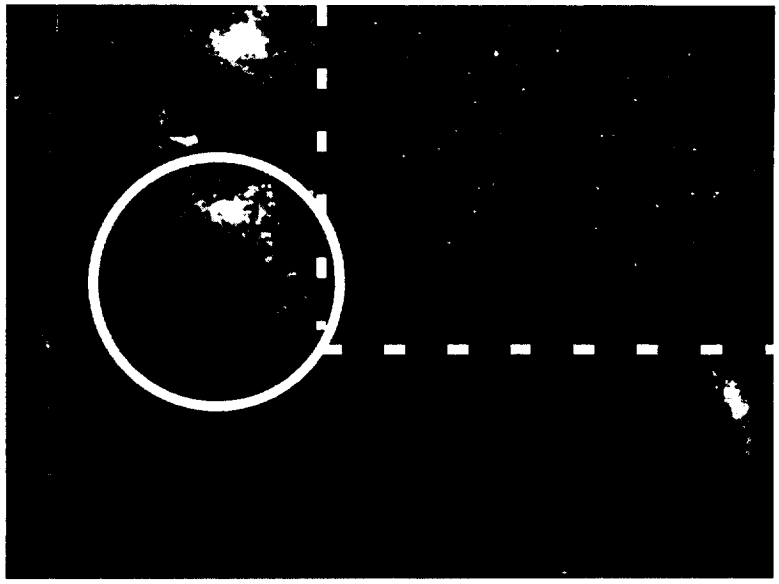

Figure 5.9 Corrosion on positive plate of 4V cell. The dashed line marks the edge of the Positive Active material (PbO_2), which has been removed. Note the corrosion marked by the circle.

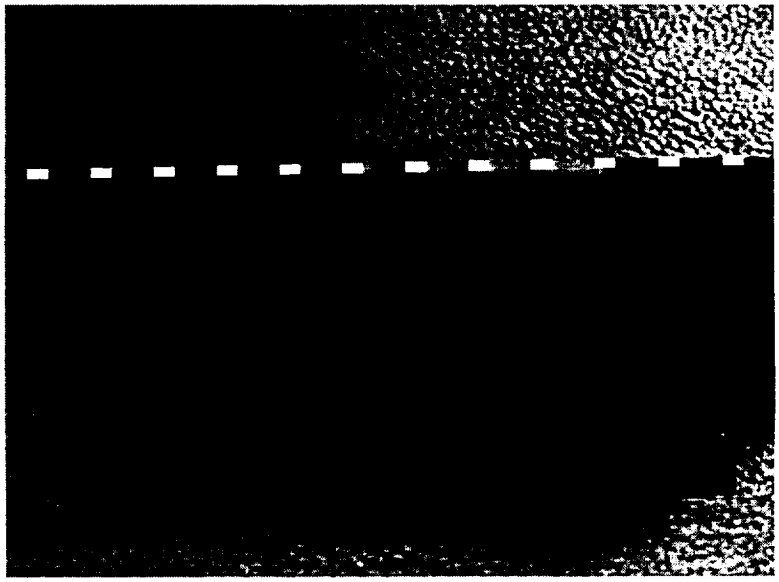

Figure 5.10 Pull-apart testing of positive side of plate revealing weakest part of plate. The plate was cut in half along the dashed line.

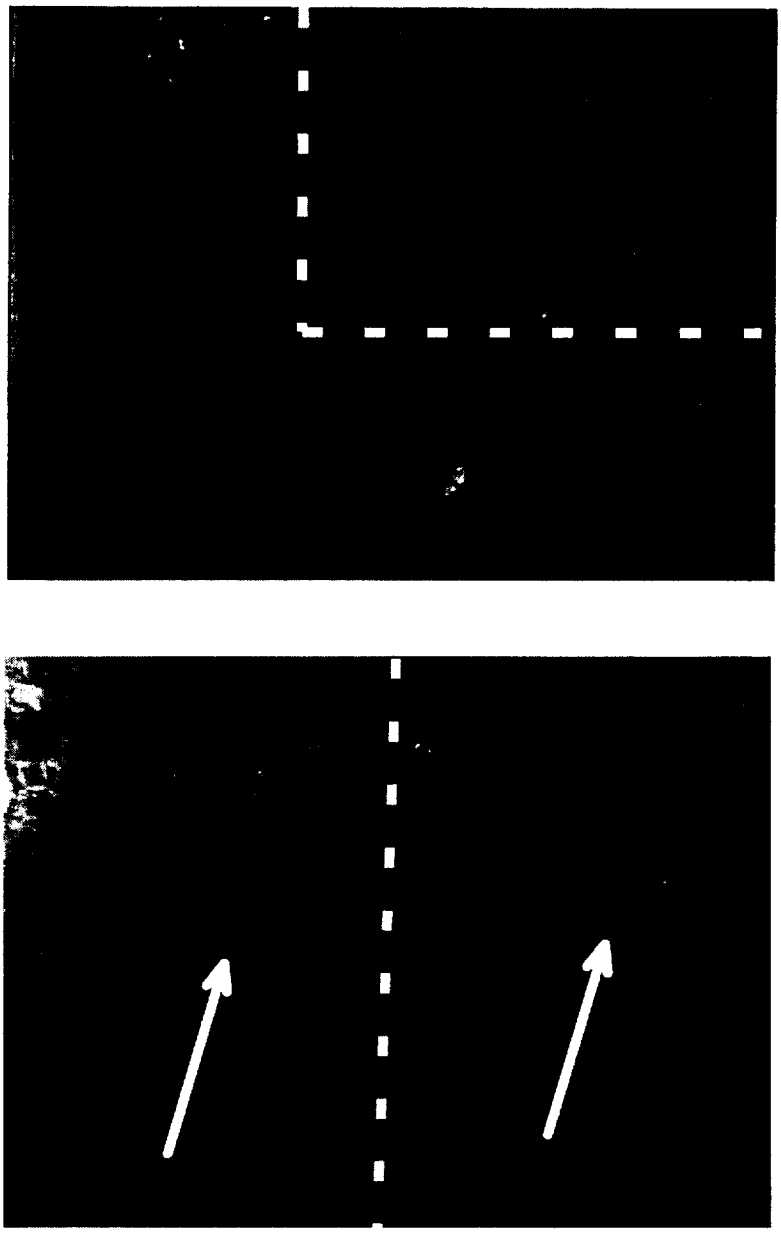

Figure 5.11 Corrosion (or lack thereof) on negative side of the 4V cell. Top: Near corner, bottom: image of seam, barely perceptible, is located by arrows. The dashed line marks the edge of the negative active material (Pb), which has been removed. No significant corrosion was observed.

5.4 Absorption of sealing material in molding/casting process.

The questions arose as to whether the separator material would wick and absorb an undue amount of the sealing material into its fibers.

The edge of a microporous separator were dipped into an epoxy compound and also a liquid plastic ("PlastiDip") sealing compound.

As can be seen in Figure 5.12, the absorption of the epoxy is limited to the edge of the microporous separator. The epoxy did not penetrate deeply into the separator because of its relatively high viscosity.

In Figure 5.13, where the separator edge has been dipped into a plastic compound, there was no significant penetration of the sealing material into the separator.

Wicking of the seal material can be controlled by either coating the separator edges with a non-penetrating compound, or by controlling the viscosity and pressure of the molding process.

Since it is clear that this is not a "show-stopper," further investigation under Phase I was not considered necessary.

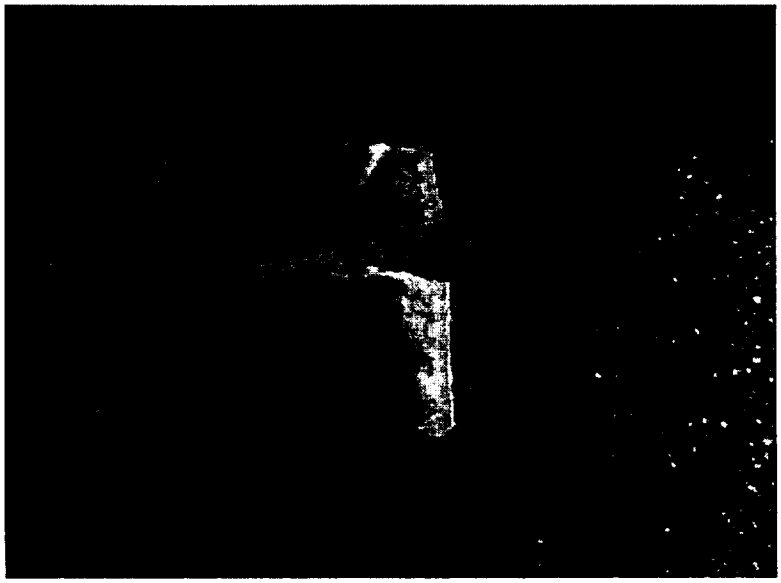

Figure 5.12 Absorption of epoxy into microporous separator edge. Note edge of separator is saturated.

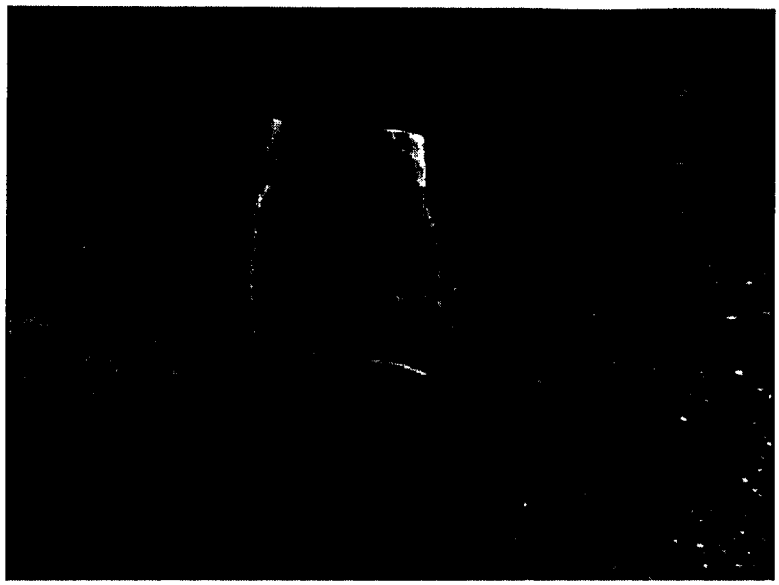

Figure 5.13 Absorption of rubber/plastic compounds into microporous separator. Note edge of separator is just coated.

Section 6

QUASI-BIPOLAR BATTERY DESIGN

Using the above models and data, hypothetical quasi-bipolar batteries were designed with realistic specifications, performance and packaging. Using the standard "baseline" performance specifications, the "~Gen2" battery pack were designed to approximate a "Gen2" hybrid-electric vehicle battery pack using Optima batteries, with the idealization that the cells are made using lead foil grids.

Three battery packs were designed. The, first "QB1," maximized the energy density of the battery using the ~Gen2 paste specifications in Table 4.2. Constraints to the optimization, are indicated in the Table by the "•" symbol. The second "QB2" was optimized for minimum thermal variation. The third, "QB3" used the high utilization paste in Table 4.2 to design a battery with excellent thermal variation, and electrical performance.

6.1 Baseline Battery Pack Thermal Characteristics

Based on a baseline stack with 168, 1.3mΩ, 0.05m diameter by 0.12m long, spiral wound cells, the cooling power requirement, as a function of the specified temperature rises, in the range 1 to 10K, of the coolant air is approximated by,

$$Pwr \sim \frac{142/W}{\left(dT_{i/o}/K\right)^3}. \tag{6.1}$$

Note that this power does not include any pressure drops through the rest of the system, nor inefficiencies in the blower. The associated log-mean temperature difference between the coolant and the battery casing is,

$$dT_{lm} \sim 0.23dT_{i/o} + 1.71K, \tag{6.2}$$

and the internal temperature variation is,

$$dT_{\text{int}\,emal} \sim 0.4K. \tag{6.3}$$

Allowing an arbitrary maximum of 0.05% of the average stack power (50 W) to go to cell cooling yields the following specifications:

$$Pwr = 50W,\ dT_{\text{int}\,emal} \sim 0.4K,\ dT_{i/o} = 1.4K \text{ and } dT_{lm} = 2.0K. \tag{6.4}$$

6.2 QB Plate parameters

The plates in this study were constructed from 0.005" thick lead foil wrapped around 0.005" thick polyester (Mylar) film. The peripheral seal depth was set to 0.2".

6.2 Observations

The QB1 battery was designed to match the thermal variation, voltage, power, and cooling power of the ~Gen2 pack, while optimizing for maximum energy density. As can be seen from Table 6.1 the QB battery has far less dead weight (see the "% total mass in active materials" item). The result is a significantly higher energy density and specific power.

The QB2 battery was designed to match only the coolant power and voltage of the ~Gen2 battery pack. It also has the restriction that it must fit in a 100L container with no dimension (L,W,H) exceeding 1.5m. The optimization was to minimize thermal variation within the cell. The result was a battery with virtually no thermal variation.

Both QB1 and QB2 have predicted performance (in all tabulated values) superior to the ~Gen2 stack. The value of thermal uniformity on battery life and performance is known to be true, but it has not been quantified. As a result, choosing between the extremes of QB1 and QB2 is not obvious.

A third battery was designed "QB3" using a (hypothetical) high utilization paste. The battery parameters were, balancing power, energy, and thermal uniformity. The result was a battery with very good thermal uniformity, high power, and moderate energy storage.

	Units	~Gen 2	QB1	QB2	QB3
Design For		-	Max Energy Density	Min Thermal Variation	Balanced High Utilization
Standard Measures					
Power Density	W/L	1,587	•	2,471	1800
Specific Power	W/kg	518	•	1,416	700
Energy Density	Wh/L	90	122	57	121
Specific Energy	Wh/kg	29	39	33	47
Number of Cells		168	•	•	•
Mass	kg	193	•	174.4	250
Volume	L	63	61.6	100	97
Active Materials:					
Assumed Utilization	%	33	•	•	50
Specific Energy of Active Materials + Sep	Wh/kg	54	•	•	70
% of Total Mass in Active Materials	%	54	72	60	68
Dimensions					
length (150cm max)	cm	-	89	150	137
width	cm	-	11	17	12
height	cm	-	63	40	60
Electrical					
Current Uniformity		0.96	0.98	0.98	0.98
A-h storage	A-h	16.5	21.9	•	34.3
Cell Resistance (mΩ)	mΩ	1.3	1.0	0.48	0.67
2/3 V_0^2/4R Power (kW)	kW	100	•	247	175
Current Density	A/cm^2	0.04	•	0.03	0.02
Thermal					
Coolant Fluid	-	Air	•	•	•
Coolant Direction	-	Axial	Normal	Normal	Normal
Average Coolant Power Draw	kW	10	•	•	•
Cooling Power	W	50	•	•	5
dT log mean to coolant	°C	2.0	1.1	2.3	1.5
dT Coolant (out-in)	°C	1.4	1.7	0.05	0.6
dT Internal	°C	0.4	0.1	0.03	0.04
dT Max	°C	1.8	•	0.08	0.6

Table 6.1 A comparison of three quasi-bipolar designs compared with the ~Gen2 battery pack. The "•" symbol means the value is the same as the ~Gen2 design.

Section 7

DISCUSSION AND RECOMMENDATIONS

Conceptually, the quasi-bipolar battery solves the through-plate failure mechanism of the true bipolar battery while retaining most of its benefits. The modeling/battery design described above demonstrates that a quasi-bipolar battery can be designed that meets or exceeds the current state-of-the-art in hybrid-electric battery pack performance. The quasi-bipolar battery potentially exhibits roughly one tenth the thermal variation expected in the state-of-the-art pack. At the same time, it has slightly lower current density. The high thermal uniformity and lower current density are factors linked to longer battery life.

The present modeling/battery design study demonstrates that there is a trade-off between thermal and specified electrical performance. Even with these tradeoffs, quasi-bipolar batteries can be designed that meet or exceed current state-of-the-art hybrid-electric vehicle battery pack electrical performance. At the same time, the battery configuration exhibits greater than ten times better thermal uniformity than state-of-the-art hybrid-electric battery packs. Thermal uniformity, power, and energy for these quasi-bipolar battery packs is projected to be very good. As shown below,

	Spiral Wound	*Max Energy Density*	*Min Thermal Variation*	*Optimistic Balanced*
Assumed Utilization of Active Materials (%)	33	33	33	50
Specific Power (W/kg)	500	500	1400	700
Power Density (W/L)	1600	1600	2500	1800
Specific Energy (Wh/kg)	29	39	33	47
Energy Density (Wh/L)	90	122	57	121
W-h battery/W-h AM (%)	54	72	60	68
Thermal dT (°C)	1.8	1.8	0.08	0.6

The batteries made from the 33% utilization active materials are representative of what can be achieved today. The optimistic balanced battery assumes a 50% utilization of the active materials. Values for the cell geometry were chosen to provide a balance between power, energy, and thermal uniformity.

The experimental part of the investigation demonstrated the concept of the quasi-bipolar plate applied to a lead foil current collector "grid" material wrapping around two sides of an inexpensive plastic film core. Approximately 50 quasi-biplate samples were fabricated using a hot laminating press. Fabrication of these plates was found to be relatively straightforward. Five of these plates were assembled into two cells plus one two-cell battery. Data from these test cells were compared with existing data for similar

true bipolar batteries. Formation and cycling of the battery caused the positive side of the plate to have a stress-corrosion problem where it was not protected by seal or active material. This problem was worst on the two cell battery where the biplate was not supported and allowed to droop around the edges. Adhesion with plastic is difficult, but hot lamination with "texture" between the plastic and lead shows some promise as a low cost method for fabricating the plates.

Further investigation of this battery could take several paths. One would be to build more prototypes, experimenting with seals (which have not been addressed at all in the present study), thicker grid materials under the seals, and other quasi biplates grids and cores. Another path would be to quantify the effect of thermal and current nonuniformity on life, and then design a battery pack for optimal life.

The next steps would benefit from some collaboration with battery manufacturer or individuals who have experience developing batteries (in particular with seals on biplates and plate corrosion).

The thermal and electrical performance of the quasi-bipolar battery presented here is predicted to be superior to the state-of-the-art spiral wound battery pack. However, the spiral wound battery is a mature technology and the thermal uniformity is pretty good. In addition, there is still room for improvement of its thermal uniformity (if that is made a priority). Whether it is worth the development effort for a relatively unproven technology like the quasi-bipolar battery stack when a good relatively mature technology is available is not yet clear. There is still the issue of premature capacity loss experienced by state-of-the-art batteries on hybrid-electric vehicle cycles. This is related to sulfitization that starts on the bottom of the negative electrode, where the current density is lower than in the rest of the plate. The quasi-bipolar plate has excellent current uniformity, and might perform better in this respect.

Another interesting concept which merits consideration, and has come up in the course of discussion of this battery on a number of occasions, is the possibility of applying the quasi-bipolar battery concept to lithium ion batteries, basically to reduce weight and cost of cell interconnections.

Section 8

ACKNOWLEDGMENTS

We would like to thank Tom Miller of NASA Lewis Research Center, John Dunning of General Motors North American Operations, and Blake Dickenson of AeroVironment, Inc. for their valuable inputs. We would also like to thank Jeff Arias, Eldon Drake, Rod Lighthipe, and Jack Rowlette of Arias Research Associates, Inc., for their discussions, and significant assistance in fabrication and testing of the quasi-bipolar test cells.

Section 9

REFERENCES

Arias Research Associates, Inc., "Hybrid Electric Vehicle Battery Development, Phase I Final Report," (Two Volumes), 1996, June 5, Document No. 33-D15. *Protected Hybrid Vehicle Information.*

The ASM Committee on Corrosion of Electrochemical Power Sources, "Corrosion in Batteries and Fuel-Cell Power Sources," pp1317-1318.

Bagshaw, N.E., "Lead alloys: past, present and future," 1995, *Journal of Power Sources* **53** pp. 25-30.

Bode, H., Lead Acid Batteries, 1977, (Brodd, R.J. and Kordesch, K.V. Trans.), John Wiley and Sons.

Crompton, T.R., Battery Reference Book, Second Edition, SAE International, 1996.

Dacres, C.M., Sutula, R.A., and Larrick, B.F., "A Comparison of Procedures Used in Assessing the Anodic Corrosion of Metal Matrix Composites and Lead Alloys for use in Lead Acid Batteries," 1983, *J. Electrochem. Soc.*, Vol. 130, No. 5, May, pp. 981-985.

DeMarco, R., "Influence of lead (II) carbonate films of non-antimonial grids on the deep discharge cycling behavior of maintenance-free lead/acid batteries," 1977, Chapman & Hall.

Dickenson, B., "Apparent Capacity Loss," 1997, March 18, EMC Data Memo. *Protected Hybrid Vehicle Information.*

ElectroSource, Inc., "Horizon Advanced Battery Technical Summary," 1995.

Gibbard, H.F., "Ultra-High-Power Batteries," 1986, *Proc. of the Symposium on Electrochemical and Thermal Modeling of Battery, Fuel Cell, and Photoenergy Conversion, The Electrochemical Society, Inc.*, Proceedings Volume 86-12, pp.193-205.

Harb, J.N., and LaFollette, M., "Mathematical Model of a Spirally-Wound Lead-Acid Cell (Final Report)," Bipolar Technologies, Provo, Utah. *Protected Hybrid Vehicle Information.*

Hosking, D., "Developments in lead/acid stationary batteries," 1993, J. Power. Sources, 45, pp. 111-117.Incorpera, F. P., and DeWitt, D. P., Fundamentals of Heat Transfer, 1981, John Wiley & Sons, New York.

Incorpera, F. P., and DeWitt, D. P., Fundamentals of Heat Transfer, 1981, John Wiley & Sons, New York.

Kays, W. M., and London, A. L., Compact Heat Exchangers, 1964, McGraw-Hill, New York.

LaFollette, R.M., and Bennion, D.N., "Design Fundamentals of High Power Density Pulsed Discharge Lead Acid Batteries I. Experimental," 1990, *J. Electrochemical Society,* **137**, No, 12, December, pp. 3693-3701.

LaFollette, R.M., and Bennion, D.N., "Design Fundamentals of High Power Density Pulsed Discharge Lead Acid Batteries II. Modelling," 1990, *J. Electrochemical Society,* **137**, No, 12, December, pp.3701-3707.

Lazarides, C., and Hampson, N.A., "On the Cycling of Positive Plante' Electrodes," 1983, J. Power Sources, 9, pp.47-54.Lee, J. "Battery Thermal Modeling - The Methodology and Applications," 1986, *Proc. of the Symposium on Electrochemical and Thermal Modeling of Battery, Fuel Cell, and Photoenergy Conversion, The Electrochemical Society, Inc.,* Proceedings Volume 86-12, pp.206-215.

Linden, D. ed., Handbook of batteries and fuel cells, 1984, McGraw-Hill.

The Materials Information Society Metals Handbook (Tenth Edition, Volume 2),.

Mattesco, P., Bui, N., Simon, P., and Albert, L., "*In Situ* Conductivity Study of the Corrosion Layers on Lead-Tin Alloys in Sulfuric Acid," 1977, J. Electr4oChemical Soc. Vol. 144, No. 2, February, 443-449.

McClintock, F.A. and Argon, A.S. ed. Mechanical Behavior of Materials, 1966, Addison-Wesley Publishing Co., Reading Massachusets.

Nakayama, Y., Obata, Atsuomi, Hojo, E., Matsumoto, N., "Development of VRLA Battery for Low Emission Hybrid Vehicle,"

Pavlov, D., Dimitrov, M., Petkov, G., Giess, H., and Gnehm, C., "The Effect on the Electrochemical Behavior and Corrosion of Pb-Sn Alloys Used in Lead-Acid Batteries," 1995, J. Electrochem. Soc., Bvol. 142, No. 9, September, pp.2919-2927.

Perry, R. H., Chilton, C. H., Chemical Engineers' Handbook, 5th Edition, 1973, McGraw-Hill, New York.

Proceedings of Second ALABC Members & Contractors Conference, 19-22 Febraury 1996, Volume 3, Sacramento, CA.

Rippel W.E., "Analysis of Battery Internal Resistance," July 15, 1994, Personal Document.

Rosato, Donald V., Plastics processing data handbook, 1990.

Rowlette, J.J., "Development Status of the ARA Sealed Bipolar Lead-Acid Battery," 1993, *Proc. of the Eighth Annual Battery Conference on Applications and Advances*, Cal. State Univ., Long Beach, Jan. 12-14.

Saxman, D., "The U.S. Battery Industry: Developing Technologies and Markets," 1994, Document GB-086N, Business Communications Company, INC. Norwalk CT.

Sheppard, L., "Gen. 2 Heater Battery Air Cooling Tests," 1997, July 25, EMC Data Memo 114-xxx. *Protected Hybrid Vehicle Information.*

Sheppard, L. "Cooling Jet Plume Area for Gen 2 Battery Air Cooling," 1977, May 15, EMC Data Memo 114-xxx. *Protected Hybrid Vehicle Information.*

Sunu, W.G., and B.W. Burrows, "Mathematical Model for Design of Battery Electrodes: II Current Density Distribution," 1984, *Proc. of the Symposium on Porous Electrodes: Theory and Practice, The Electrochemical Society, Inc.*, Proceedings Voume 84-4, pp. 462-481.

Young, J.F., Shane, R.S., Ed. Materials and Processes (Third Edition, Part A:Materials), 1985, Marcel Dekker, Inc, New York.

REPORT DOCUMENTATION PAGE

Form Approved
OMB No. 0704-0188

1. AGENCY USE ONLY (*Leave Blank*)	2. REPORT DATE	3. REPORT TYPE AND DATES COVERED
	15 Jan 98	FINAL, 1 July 97 - 31 Dec 97

4. TITLE AND SUBTITLE
Development of a Woven-Grid Quasi-BiPolar Battery

5. FUNDING NUMBERS
NAS3-97164

6. AUTHOR(S)
P. Tokumaru, Ph.D.
W. Rippel
T. Zambrano

7. PERFORMING ORGANIZATION NAME(S) AND ADDRESS(ES)
AeroVironment Inc.
222 E. Huntington Drive, Ste. 200
Monrovia, CA 91016

8. PERFORMING ORGANIZATION REPORT NUMBER
AV-AS100060

9. SPONSORING/MONITORING AGENCY NAME(S) AND ADDRESS(ES)
Supported by Ballistic Missile Defense Organizational Science and Technology and managed by
NASA Lewis Research Center
Procurement/MS 500-306
Cleveland, Ohio 44135-3191

10. SPONSORING/MONITORING AGENCY REPORT NUMBER

11. SUPPLEMENTARY NOTES

12a. DISTRIBUTION/AVAILABILITY STATEMENT
Approved for public release; distribution unlimited

12b. DISTRIBUTION CODE

13. ABSTRACT (*Maximum 200 words*)

This report describes an analytical and experimental investigation of AeroVironment's Quasi-Bipolar battery concept.

The modelling/battery design part of the study demonstrates that there is a trade-off between thermal and specified electrical performance. Even so, quasi-bipolar batteries can be designed, with ten times better thermal uniformity, that meet or exceed current state-of-the-art hybrid-electric vehicle battery pack performance, even using the same active materials. The thermal uniformity, power, and energy for these quasi-bipolar battery packs is projected to be very good.

The experimental part of the investigation demonstrates the concept of the quasi-bipolar plate applied to a lead foil current collector wrapping around two sides of an inexpensive plastic film core. Approximately 50 quasi-biplate samples were fabricated using a hot laminating press. Hot lamination with "texture" between the plastic and lead shows some promise as a low cost method for fabricating the plates. Five of these plates were assembled into two cells plus one two-cell battery. Data from these test cells were compared with existing data for similar true bipolar batteries. The positive side of the plates exhibited corrosion where not protected by the active material.

14. SUBJECT TERMS

15. NUMBER OF PAGES

16. PRICE CODE

17. SECURITY CLASSIFICATION OF REPORT	18. SECURITY CLASSIFICATION OF THIS PAGE	19. SECURITY CLASSIFICATION OF ABSTRACT	20. LIMITATION OF ABSTRACT
UNCLASSIFIED			UL